Image noise reduction based on applying adaptive thresholding onto PDEs methods

Ali Abdullah Yahya[1], Jieqing Tan[2], Benyu Su[1], Kui Liu[1], Ali Naser Hadi[2]

[1]*School of Computer and Information, Anqing Normal University, Anqing 246011, People's Republic of China*
[2]*School of Computer and Information, Hefei University of Technology, Hefei 230009, People's Republic of China*
E-mail: aselwey1@hotmail.com

Published in *The Journal of Engineering*; Received on 4th April 2017; Accepted on 26th April 2017

Abstract: In this study the authors present a novel image denoising method based on applying adaptive thresholding on partial differential (PDEs) methods. In the proposed method the authors utilise the adaptive thresholding to blend the total variation filter with anisotropic diffusion filter. The adaptive thresholding has a high capacity to adapt and change according to the amount of noise. More specifically, applying a hard thresholding on the higher noise areas, whereas, applying soft thresholding on the lower noise areas. Therefore, the authors can successfully remove the noise effectively and maintain the edges of the image simultaneously. Based on the adaptation and stability of the adaptive thresholding we can achieve; optimal noise reduction and sharp edges as well. Experimental results demonstrate that the new algorithm consistently outperforms other reference methods in terms of noise removal and edges preservation, in addition to 4.7 dB gain higher than those in the other reference algorithms.

1 Introduction

Image denosing is a major step in all of computer vision and image processing systems. Since the noise is related to high frequencies, it is too difficult to eliminate this noise, and at the same time maintaining the significant image features (e.g. edges) [1].

Image denoising plays an important role in guaranteeing the effectiveness and sturdiness of image processing algorithms in the industry image process procedures, for instance; image registration, image segmentation. For that reason image denoising is still attracting a considerable attention of the researchers [2]. Several methods have been proposed in the literature to address the problem of image denoising, most notably; partial differential equation (PDE) methods [3–5], transform-domain methods [6], Gaussian smoothing method [7], Gabor filtering method [8], empirical Wiener filter [9] and wavelet thresholding method [10].

In the recent decades, PDEs became an important approach of image denoising. The strategy of PDEs-based methods is to distort a given image with a PDE and solve this equation to get the denoised image [11].

The oldest PDE filtering model is the linear heat equation. This equation diffuses in one dimension which will lead to get a smooth image, but unfortunately fails to preserve the significant information of the image (e.g. edges).

The second-order non-linear PDE models have been proposed to avoid this flaw of the heat equation [12]. The most popular non-linear filtration methods that based on PDE are; total variation (TV) and anisotropic diffusion [Perona and Malik (PM)].

Anisotropic diffusion filter has been proposed in 1990 by Perona and Malik (PM) [3]. In anisotropic diffusion model the rate of diffusion is controlled by edge stopping function. This filter is useful tool for multi-scale description of images, image segmentation, edge detection, and image enhancement. In this filter, an anisotropic diffusion equation has been used to smooth the degraded image. The basic idea of the anisotropic diffusion equation is to increase smoothness within the regions attained through pre-estimation, whilst less smoothness across edges, to get sharper and more defined edges [11]. Nevertheless, the serious disadvantage of anisotropic diffusion model is that the sharp edges and fine details are not preserved well during noise removal process. To treat this drawback Kamalaveni *et al.* [13] proposed to use appropriate edge stopping function.

Yang *et al.* [14] adopted non-local means theory to improve anisotropic diffusion model. The authors assumed that the image contains an extensive amount of self-similarity. In this model, the similarity between the region around the centre pixel and the region outside the centre pixel has been used to give a more reasonable description of the image.

The second popular model of PDEs-based approaches is the TV model. This model was first proposed by Rudin *et al.* [5] for edge-preserving and noise removal. In this model, the following equation has been proposed to smooth the image and preserve the edges and details: $E(u) = \int\int_{\Omega} [|\nabla u| + \lambda(u - u_0)^2]\mathrm{d}x\mathrm{d}y$. This model has the potential to handle the edges and eliminate noise in a given image. TV model is a good in terms of maintaining the edges, however, this model can cause the staircase effect and loss the image structure as well as texture information. To obviate these drawbacks, Lysaker and Tai [15], proposed to combine TV minimisation and a fourth-order PDE filter.

So many researchers tried to combine TV filter with anisotropic diffusion filter for image denoising in order to make full use of the denoising advantages of these two models.

In this paper we use an adaptive thresholding (soft and hard thresholding) to combine the TV model and anisotropic diffusion model. The proposed adaptive thresholding has the ability to adapt and change in each area according to the area information (flat area or edges). More accurately, applying the hard-thresholding to the flat areas which contain less image features and much noise, will allow us to remove noise very effective. Whereas applying the soft-thresholding to the areas which contain more image features will allow us to maintain the image features such as edges.

The remainder of this paper is organised as follows. In Section 2, we briefly describe the TV and anisotropic diffusion filters. The proposed model is described in Section 3. The experimental results are presented in Section 4. Some concluding remarks are outlined in Section 5.

2 Anisotropic diffusion and total variation filters

2.1 Anisotropic diffusion filter

In last few decades, image denoising methods based on partial differential equation have been developed extensively. One of the most famous image denoising approach based on partial differential equation is anisotropic diffusion model which was first proposed by Perona and Malik [3]. In this model, the linear (heat) equation was replaced by a non-linear diffusion equation which is commonly used in the fields of image denoising and enhancement.

Perona and Malik [3] adopted the diffusion coefficient which is small while the gradient of image is large to control the diffusivity at those locations which have a larger likelihood to be edges.

Perona–Malik filter based on the following equation:

$$\frac{\partial f}{\partial t} = \operatorname{div}(g(|\nabla f|)\nabla f), \tag{1}$$

and the diffusivity function is given by

$$g(|\nabla f|) = \frac{1}{1 + (|\nabla f|^2/k^2)}, k > 0, \tag{2}$$

where $g(|\nabla f|)$ is a monotone decreasing smooth function with:

$$\lim_{|\nabla f| \to 0} g(|\nabla f|) = 1, \tag{3}$$

fast-diffusion.

And

$$\lim_{|\nabla f| \to \infty} g(|\nabla f|) = 0, \tag{4}$$

slow or stopped diffusion.

From (3) and (4) we can observe that the diffusion is high as the gradient is small, which results in more smoothing in the flat area of the image. Whereas, the diffusion will be low as the gradient is large, which results in less smoothing in the edges of the image [14].

To get reconstruction f of a degraded image f_0, Weickert [16] used the following energy function:

$$E(f) = \int\int_{\Omega} \left(\lambda(f - f_0)^2 + k^2 \ln\left(\frac{1}{g(|\nabla f|)} \right) \right) \mathrm{d}x\mathrm{d}y, \tag{5}$$

and the corresponding Euler Lagrange equation will be as follows:

$$-\nabla \cdot (g(|\nabla f|)\nabla f) + 2\lambda(f - f_0) = 0. \tag{6}$$

A general expression of the anisotropic diffusion equation which was first proposed by Perona and Malik can be written as follows [17]:

$$\begin{cases} \dfrac{\partial u}{\partial t} = \nabla \cdot (g(|\nabla f|)\nabla f) - 2\lambda(f - f_0), \\ \quad [\text{where } \nabla \cdot (g(|\nabla f|)\nabla f) \text{ in } \Omega \times (0, T)] \\ \dfrac{\partial f}{\partial n} = 0 \text{ on } \partial\Omega \times (0, T) \\ f(x, y, t)|_{t=0} = f_0(x, y) \text{ in } \Omega, \end{cases} \tag{7}$$

where $f(x, y, t)|_{t=0} = f_0(x, y)$ is the initial condition and Ω is an open bounded domain in $\mathbb{R}^2$.

The anisotropic diffusion model has the high capacity to remove the noise very well. Nevertheless, this model suffers from ill-posed problem, in other words, the existence and uniqueness of the solution of (7) cannot be guaranteed, therefore, when the noise and edge have the same gradient, formula (7) will fail to be applied for de-noising. Hence, it is highly likely that this model can cause Gibbs-type artefacts.

2.2 *Total variation filter*

In 1992 Rudin, Osher and Fatemi (ROF) proposed a successful minimisation approach to retrieve images with sharp edges. In this approach the L^2 norm which was proposed by Tikhonov and Arsenin [18] has been replaced by L^1 norm of the gradient of f.

To recover the original image, ROF proposed to minimise the TV as follows:

$$\mathrm{TV}(f) = \int\int_{\Omega} |\nabla f| \mathrm{d}x\mathrm{d}y, \tag{8}$$

subject to

$$\int\int_{\Omega} f(x, y)\mathrm{d}x\mathrm{d}y = \int\int_{\Omega} f_0(x, y)\mathrm{d}x\mathrm{d}y, \tag{9}$$

$$\frac{1}{|\Omega|}\int\int_{\Omega} (f(x, y) - f_0(x, y))^2 \mathrm{d}x\mathrm{d}y = \sigma^2, \tag{10}$$

where f and f_0 represent original and degraded images, respectively. In (10) the additive noise $n(x, y)$ is of zero mean and has known variance σ^2. By introducing Lagrange multiplier λ, the energy function of the image can be defined as:

$$E(f) = \int\int_{\Omega} [|\nabla f| + \lambda(f - f_0)^2] \mathrm{d}x\mathrm{d}y. \tag{11}$$

In this paper we will adopt the PDEs methods to solve the above constrained variational problem.

Solutions of (8)–(10) necessarily achieve the following Euler-Lagrange equation:

$$-\nabla \cdot \left(\frac{\nabla f}{|\nabla f|} \right) + 2\lambda(f - f_0) = 0. \tag{12}$$

By the gradient descent method, we can obtain the TV denoising model [19]:

$$\begin{cases} \dfrac{\partial f}{\partial t} = \left(\nabla \cdot \left(\dfrac{\nabla f}{|\nabla f|} \right) - 2\lambda(f - f_0) \right), \\ \quad [\text{where } \nabla \cdot \left(\dfrac{\nabla f}{|\nabla f|} \right) \text{ in } (0, \infty) \times \Omega], \\ \dfrac{\partial f}{\partial n} = 0 \text{ on } (0, \infty) \times \partial\Omega, \\ f(x, y, t)|_{t=0} = f_0(x, y) \text{ for } (x, y) \in \Omega, \end{cases} \tag{13}$$

where $f(x, y, t)|_{t=0} = f_0(x, y)$ is the initial condition and Ω is an open bounded domain in $\mathbb{R}^2$.

TV filter can effectively remove the noise without blurring image edges, by minimising the energy functional [20]. However, this model can cause staircase effect and therefore loss of image structure and texture information.

3 Proposed model

The greatest challenge that face image denoising algorithms is lying in removing the noise without blurring the edges of the image. In our proposed model, we try to address this problem by utilising the adaptive thresholding to distinguish between flat areas and edges. More precisely, less noise removal on the edges of the image, and more removal in the lflat areas.

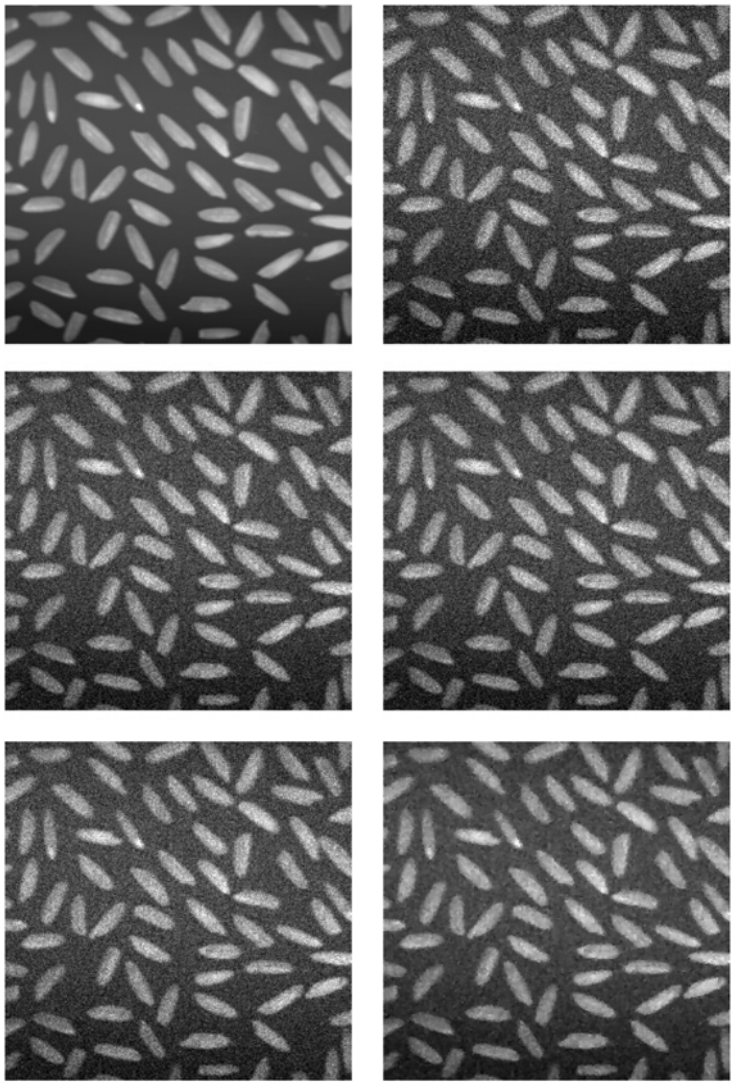

Fig. 1 *Results of denoising obtained with Rice image (standard deviation of additive white Gaussian noise = 20). From left- to right-hand side and from top to bottom: result of [21] algorithm, result of [22] algorithm, result of [17] algorithm, and result of the new algorithm*

Now let us take the following energy function of the image to restore the original image f from the degraded image f_0:

$$E(f) = \int\int_{\Omega}\left[S|\nabla f| + (1-S)\,k^2 \cdot \ln\left(\frac{1}{g(|\nabla u|)}\right) + \lambda(f-f_0)^2\right]\mathrm{d}x\mathrm{d}y. \tag{14}$$

where

$$S = \begin{cases} N > T1, & \text{Hard} - \text{thresholding} \\ \text{Otherwise} & \text{Soft} - \text{thresholding} \end{cases} \tag{15}$$

where N is the standard deviation/variance of noise and $T1$ is selected thresholds.

In this paper the soft thresholding formulation is:

$$X_{\text{soft}} = \begin{cases} \text{sign}(X)(|X| - T) & \text{if } |X| > T, \\ 0 & \text{if } X \le T, \end{cases} \tag{16}$$

and hard thresholding formulation is:

$$X_{\text{Hard}} = \begin{cases} X & \text{if } |X| > T, \\ 0 & \text{if } X \le T. \end{cases} \tag{17}$$

where

$$X = \frac{1}{(ex)^2 + f_x^2 + f_y^2}, \tag{18}$$

here ex is initial constant.

From (6) and (12) the corresponding Euler-Lagrange equation will be:

$$\left[-S\nabla\cdot\left(\frac{\nabla f}{|\nabla f|}\right) - (1-S)\nabla\cdot(g(|\nabla f|)\nabla f) + 2\lambda(f - f_0 + C) = 0\right]. \tag{19}$$

By using the gradient descent method, the new model can be expressed as follows:

$$\begin{cases} \left[\dfrac{\partial f}{\partial t} = S\nabla\cdot\left(\dfrac{\nabla f}{|\nabla f|}\right) + (1-S)\nabla\cdot(g(|\nabla f|)\nabla f) - 2\lambda(f - f_0)\right] \\ f(x, y, t)|_{t=0} = f_0(x, y). \end{cases} \tag{20}$$

From (20) we can expect that:

- In the region which contains more image features (such as edges etc.), the new model will play good role to preserve the edges of the

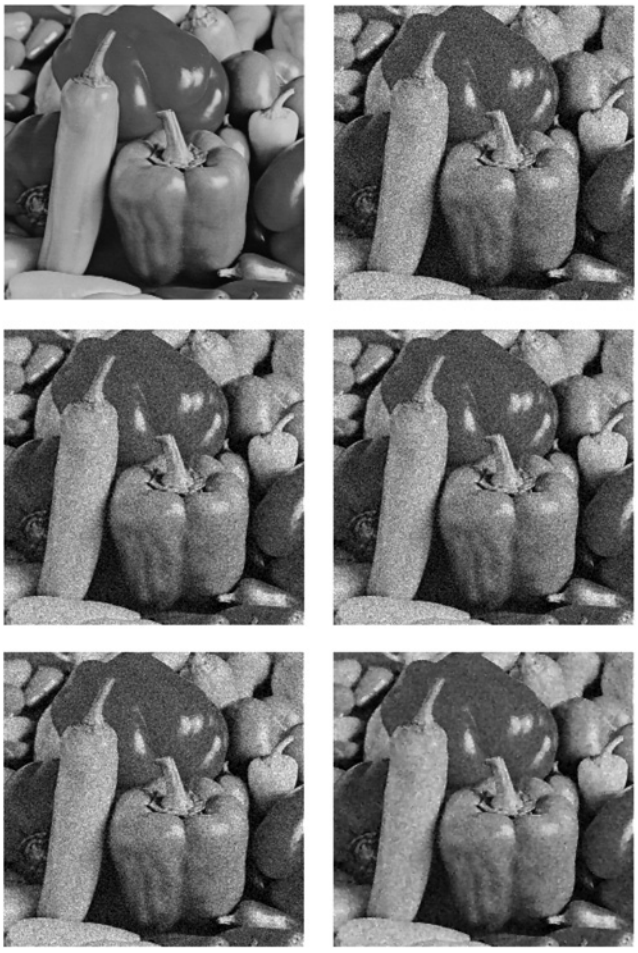

Fig. 2 *Results of denoising obtained with Pepper image (standard deviation of additive white Gaussian noise = 20). From left- to right-hand side and from top to bottom: result of [21] algorithm, result of [22] algorithm, result of [17] algorithm, and result of the new algorithm*

Fig. 3 *Results of denoising obtained with Lena image (variance of salt and pepper = 0.04). From left- to right-hand side and from top to bottom: result of [21] algorithm, result of [22] algorithm, result of [17] algorithm, and result of the new algorithm*

image, namely this model will highlight the TV model therefore S should be close to one.

- In the flat areas of image, which contains less image features, and much noise, the new model will highlight the role of the PM model, hence S should be close to zero.

To solve problem (20) by using the finite difference method, we let

$$P = \nabla \cdot (g(|\nabla f|)\nabla f), \tag{21}$$

$$T = \nabla \cdot \left(\frac{\nabla f}{|\nabla f|}\right), \tag{22}$$

Then

$$\begin{aligned} P &= \nabla \cdot (g(|\nabla f|)\nabla f) \\ &= \left(\frac{\partial}{\partial x}, \frac{\partial}{\partial y}\right) \cdot \left(\frac{f_x}{1 + ((|\nabla f|/k))^2}, \frac{f_y}{1 + ((|\nabla f|/k))^2}\right) \\ &= k^2 \left[\frac{\partial}{\partial x}\left(\frac{f_x}{k^2 + f_x^2 + f_y^2}\right) + \frac{\partial}{\partial y}\left(\frac{f_y}{k^2 + f_x^2 + f_y^2}\right)\right] \\ &= k^2 \frac{f_{xx}(k^2 + f_x^2 + f_y^2) - f_x(2f_xf_{xx} + 2f_yf_{xy})}{(k^2 + f_x^2 + f_y^2)^2} \\ &\quad + k^2 \frac{f_{yy}(k^2 + f_x^2 + f_y^2) - f_y(2f_xf_{xy} + 2f_yf_{yy})}{(k^2 + f_x^2 + f_y^2)^2} \\ &= [k^2 f_{xx} + k^2 f_{yy} - f_x^2 f_{xx} + f_y^2 f_{xx} \\ &\quad - 4f_xf_yf_{xy} + f_x^2 f_{yy} - f_y^2 f_{yy}]/\left(\frac{k^2 + f_x^2 + f_y^2}{k}\right)^2, \end{aligned}$$

$$\begin{aligned} T &= \nabla \cdot \left(\frac{\nabla f}{|\nabla f|}\right) \\ &= \left(\frac{\partial}{\partial x}, \frac{\partial}{\partial y}\right) \cdot \left(\frac{f_x}{\sqrt{f_x^2 + f_y^2}}, \frac{f_y}{\sqrt{f_y^2 + f_y^2}}\right) \\ &= \frac{\partial}{\partial x}\left(\frac{f_x}{\sqrt{f_x^2 + f_y^2}}\right) + \frac{\partial}{\partial y}\left(\frac{f_y}{\sqrt{f_x^2 + f_y^2}}\right) \\ &= \frac{f_x^2 f_{xx} + f_y^2 f_{xx} - f_x^2 f_{xx} - f_x f_y f_{xy}}{(f_x^2 + f_y^2)^{(3/2)}} \end{aligned}$$

doi: 10.1049/joe.2017.0112

Fig. 4 *Results of denoising obtained with Cameraman image (variance of salt and pepper noise = 0.04). From left- to right-hand side and from top to bottom: result of [21] algorithm, result of [22] algorithm, result of [17] algorithm, and result of the new algorithm*

$$+\frac{f_x^2 f_{yy}+f_y^2 f_{yy}-f_x f_y f_{xy}-f_y^2 f_{yy}}{(f_x^2+f_y^2)^{(3/2)}}$$
$$=\frac{f_x^2 f_{yy}-2f_x f_y f_{xy}+f_y^2 f_{xx}}{(f_x^2+f_y^2)^{\frac{3}{2}}}.$$

Replacing the first order derivatives by central divided differences and the second order derivatives by forward divided differences, we can rewrite the new model (20) as the discrete form as follows:

$$\frac{f^{n+1}-f^n}{\Delta t}=ST^n+(1-S)P^n-2\lambda(f^n-f_0^n), \qquad (23)$$

where $n=0, 1, 2, \ldots$ is the time level.

Introducing the space discrete sign

$$\frac{f^{n+1}-f^n}{\Delta t}=\frac{f_{i,j}^{n+1}-f_{i,j}^n}{\Delta t},$$

we can further rewrite (23) as

$$f_{i,j}^{n+1}=\left(f_{i,j}^n+\Delta t[ST_{i,j}^n+(1-S)P_{i,j}^n-2\lambda(f_{i,j}^n-f_0^n)]\right), \qquad (24)$$

where

$$P_{i,j}^n=\nabla^n\cdot(g(\left|\nabla f_{i,j}^n\right|)\nabla f_{i,j}^n)$$
$$=[(k^2(f_{xx})_{i,j}^n+k^2(f_{yy})_{i,j}^n-(f_x^2)_{i,j}^n(f_{xx})_{i,j}^n+(f_y^2)_{i,j}^n(f_{xx})_{i,j}^n$$
$$-4(f_x)_{i,j}^n(f_y)_{i,j}^n(f_{xy})_{i,j}^n+(f_x^2)_{i,j}^n(f_{yy})_{i,j}^n$$
$$-(f_y^2)_{i,j}^n(f_{yy})_{i,j}^n)]/\left(\frac{k^2+(f_x^2)_{i,j}^n+(f_y^2)_{i,j}^n}{k}\right)^2,$$

$$T_{i,j}^n=\nabla^n\cdot\left(\frac{\nabla f_{i,j}^n}{\left|\nabla f_{i,j}^n\right|}\right)$$
$$=[(f_x^2)_{i,j}^n(f_{yy})_{i,j}^n-2(f_x)_{i,j}^n(f_y)_{i,j}^n(f_{xy})_{i,j}^n$$
$$+(f_y^2)_{i,j}^n(f_{xx})_{i,j}^n]/((f_x^2)_{i,j}^n+(f_y^2)_{i,j}^n)^{(3/2)},$$

where

$$(f_x)_{i,j}^n=\frac{f_{i+1,j}^n-f_{i-1,j}^n}{2\Delta x}$$
$$=\frac{f(x_i+\Delta x,y_j,t_n)-f(x_i-\Delta x,y_j,t_n)}{2\Delta x},$$

doi: 10.1049/joe.2017.0112

Table 1 PSNRs results for rice image corrupted by additive white Gaussian noise

Standard deviation (σ)	5	10	20	30	40	50	60
[21] model	35.87	29.33	22.84	19.16	16.53	14.57	12.95
[22] model	35.81	29.20	22.72	19.05	16.43	14.47	12.85
[17] model	36.04	29.38	22.85	19.15	16.52	14.54	12.91
new model	38.98	34.68	27.55	22.18	18.51	15.89	13.90

Table 2 PSNRs results for pepper image corrupted by additive white Gaussian noise

Standard deviation (σ)	5	10	20	30	40	50	60
[21] model	35.57	29.26	22.95	19.18	16.56	14.56	12.95
[22] model	35.54	29.16	22.78	19.04	16.43	14.46	12.81
[17] model	35.73	29.33	22.90	19.14	16.51	14.53	12.87
new model	35.75	33.29	27.36	22.13	18.42	15.88	13.84

Table 3 PSNRs results for Lena image corrupted by salt and pepper noise

Variance of the noise	0.01	0.02	0.04	0.06	0.08	0.1
[21] model	27.32	24.23	21.08	18.95	17.60	16.54
[22] model	27.29	24.19	21.04	18.91	17.56	16.49
[17] model	27.52	24.41	21.24	19.09	17.73	16.65
new model	31.13	28.83	25.47	22.70	20.98	19.51

Table 4 PSNRs results for cameraman image corrupted by salt and pepper noise

Variance of the noise	0.01	0.02	0.04	0.06	0.08	0.1
[21] model	28.25	25.16	22.01	19.89	18.16	16.95
[22] model	28.23	25.14	21.98	19.88	18.14	16.93
[17] model	28.48	25.37	22.19	20.06	18.29	17.08
new model	30.08	28.10	25.09	22.79	20.60	19.24

$$
\begin{aligned}
(f_y)_{i,j}^n &= \frac{f_{i,j+1}^n - f_{i,j-1}^n}{2\Delta y} \\
&= \frac{f(x_i, y_j + \Delta y, t_n) - f(x_i, y_j - \Delta y, t_n)}{2\Delta y}, \\
(f_{xx})_{i,j}^n &= \frac{f_{i+1,j}^n - 2f_{i,j}^n + f_{i-1,j}^n}{\Delta x^2}, \\
(u_{yy})_{i,j}^n &= \frac{f_{i,j+1}^n - 2f_{i,j}^n + f_{i,j-1}^n}{\Delta y^2}, \\
(f_{xy})_{i,j}^n &= \frac{f_{i+1,j+1}^n - f_{i+1,j-1}^n}{4\Delta x \Delta y} \\
&\quad + \frac{-f_{i-1,j+1}^n + f_{i-1,j-1}^n}{4\Delta x \Delta y}.
\end{aligned}
$$

4 Experimental results and analysis

In this section, we verify the efficiency of the proposed filer by selecting different types of common images, and use additive white Gaussian noise and salt and pepper noise to contaminate these images. Then, we apply four different filters to remove these noise as shown in Figs. 1–4, where in each figure are elucidated, respectively; original frame, noisy frame, results by: [21]

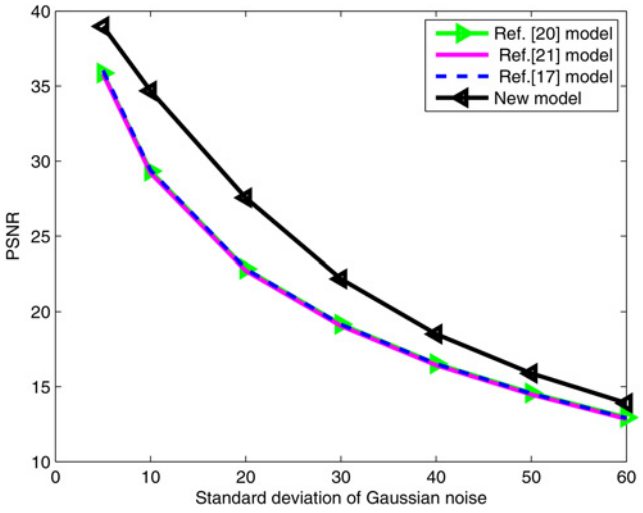

Fig. 5 *PSNR(dB) graph of [21] algorithm, [22] algorithm, [17] algorithm, and result of the new algorithm for various additive white Gaussian noise levels for Rice image*

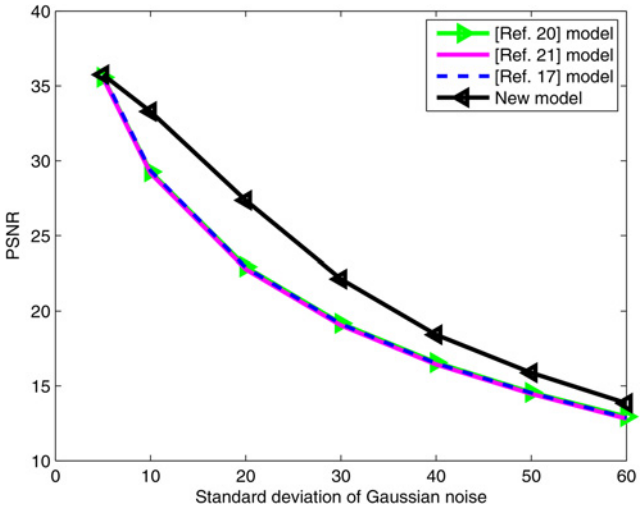

Fig. 6 *PSNR(dB) graph of [21] algorithm, [22] algorithm, [17] algorithm, and result of the new algorithm, for various additive white Gaussian noise levels for Pepper image*

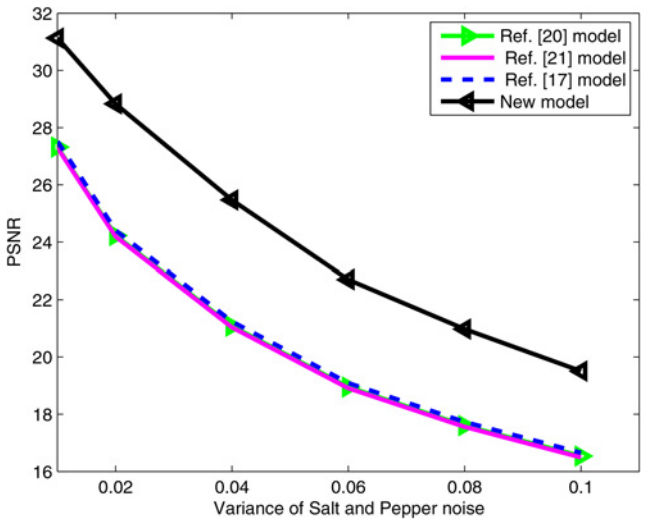

Fig. 7 *PSNR(dB) graph of [21] algorithm, [22] algorithm, [17] algorithm, and result of the new algorithm, for various salt and pepper noise levels for Lena image*

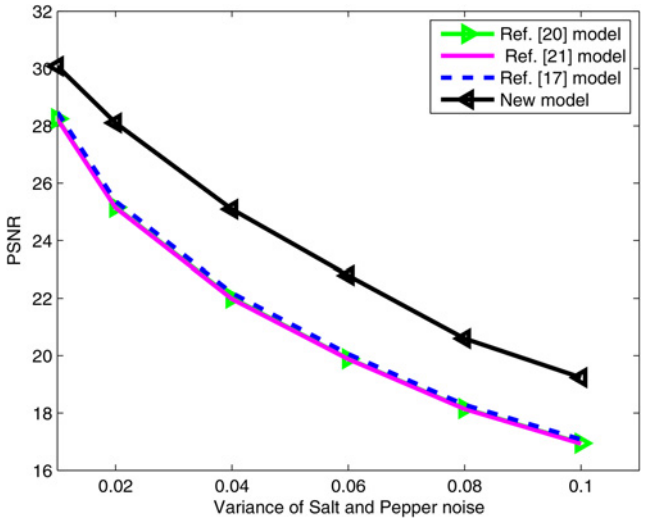

Fig. 8 *PSNR (dB) graph of [21] algorithm, [22] algorithm, [17] algorithm, and result of the new algorithm, for various salt and pepper noise levels for Cameraman image*

model, [22] model, [17] model and our new model. All of visual quality of denoised image and peak signal to noise ratio (PSNR) are used to assess the denosing effect and evaluate the edges preservation ability of our proposed method compare with other reference methods.

To demonstrate the performance's superiority of our proposed algorithm, we compare our algorithm with three related algorithms.

Figs. 1–4 show that the proposed algorithm has a very obvious denoising effect; it does not only maintain the advantages of the PM model, and TV model, but also overcomes the disadvantages of the two models. Based on Figs. 1–4, we can note that our proposed approach is very effective in terms of noise removal and edge preservation as compared with other algorithms.

Owing to applying the adaptive thresholding in the proposed algorithm, our algorithm has a high capacity to distinguish between the image textures and the noise. Unlike the algorithms in [17, 21, 22] which the detail structures and textures are often misclassified as noise.

Tables 1–4, compare the PSNR results of four different algorithms when denoising white Gaussian noise and salt and pepper images with varying standard deviation and variance ranging from $\sigma = 5 - 60$ and $\sigma^2 = 0.01 - 0.1$, respectively.

The data in Tables 1–4 demonstrate that, the proposed algorithm outperforms the algorithms in [17, 21, 22] in terms of PSNR in all experiments. Form these tables, we can note that our proposed algorithm has made a great improvement in the PSNR of the other algorithms up to 4.7 dB.

Figs. 5–8 include different values of PSNR of the four models with different noise standard deviations and variances. These figures show that, the proposed algorithm surpass all of the reference algorithms in terms of PSNR in all the noise levels.

5 Conclusion

In this paper, a novel model of image denoising based on applying adaptive thresholding to PDE filters has been presented. This model has a high potential to acclimate and change according to the amount of the noise. Accordingly, our model is able to mitigate the noise from noisy image effectively. In the proposed algorithm, we applied the adaptive thresholding, which showed high efficiency at distinguishing between the heavy noise areas and slight noise areas. Consequently, our algorithm has succeeded in preserving the details (e.g. edges) and removing the noise efficaciously in comparison with the other reference methods. The work in this paper demonstrates good denoising performance, which urges us to consider developing the existing adaptive thresholding and applying it in the future work. The experimental results with four of the most common images and various levels of white Gaussian noise and salt and pepper noise demonstrate that the proposed model has achieved good and stable denoising performance in terms of both PSNR and subjective visual quality, in addition to 4.7 dB gain higher than those in the other reference algorithms.

6 Acknowledgment

This work supported by the Natural Science Foundation of Anhui Province under grant (nos.1608085MF144 and 1608085QF131)

7 References

[1] Chatterjee P., Milanfar P.: 'Is denoising dead?', *IEEE Trans. Image Process.*, 2010, **9**, (4), pp. 895–911
[2] Huang L.: 'Improved non-local means algorithm for image denoising', *J. Comput. Commun.*, 2015, **3**, pp. 23–29
[3] Perona P., Malik J.: 'Scale-space and edge detection using anisotropic diffusion', *IEEE Trans. Pattern Anal. Mach. Intell.*, 1990, **12**, (7), pp. 629–639
[4] Bayram I., Kamasak M.E.: 'Directional total variation'. Proc. of 20th European Signal Processing Conf., 2012, pp. 265–269
[5] Rudin L., Osher S., Fatemi E.: 'Nonlinear total variation based noise removal algorithms', *Physica D*, 1992, **60**, (1-4), pp. 259–268
[6] Portilla J., Strela V., Wainwright M.J., *ET AL.*: 'Imagedenoising using scale mixtures of Gaussians in the wavelet domain', *IEEE Trans. Image Process.*, 2003, **12**, (11), pp. 1338–1351
[7] Lindenbaum M., Fischer M., Bruckstein A.: 'On Gabors contribution to image enhancement', *Pattern Recognit.*, 1994, **27**, (1), pp. 1–8
[8] Yang Y., Li B.: 'Non-linear image enhancement for digital TV applications using Gabor filters'. Proc. of IEEE Int. Conf. on Multimedia and Expo, 2005, pp. 1–4
[9] Ghael S., Sayeed A.M., Baraniuk R.G.: 'Improved wavelet denoising via empirical wiener filtering'. Proc. of SPIE, Wavelet Applications in Signal and Image Processing V, 1997, vol. **3169**, pp. 389–399
[10] Donoho D.L.: 'Denoising by soft-thresholding', *IEEE Trans. Inf. Theory*, 1995, **41**, (3), pp. 613–627
[11] Chen S., Liu M., Zhang W., *ET AL.*: 'Edge preserving image denoising with a closed form solution', *Pattern Recognit.*, 2013, **46**, (3), pp. 976–988
[12] Tang C., Han L., Ren H., *ET AL.*: 'The oriented-couple partial differential equations for filtering in wrapped phase patterns', *Opt. Soc. Am.*, 2009, **17**, (7), pp. 5606–5617

[13] Kamalaveni V., Rajalakshmi R.A., Narayanankutty K.A.: 'Image denoising using variations of Perona-Malik model with different edge stopping functions'. Proc. of Second Int. Symp. on Computer Vision and the Internet, 2015, vol. **58**, pp. 673–682
[14] Yang M., Liang J., Zhang J., *ET AL.*: 'Non-local means theory based Perona-Malik model for image denosing', *Neurocomputing*, 2013, **120**, (23), pp. 262–267
[15] Lysaker M., Tai X.-C.: 'Iterative image restoration combining total variation minimization and a second-order functional', *Int. J. Comput. Vis.*, 2006, **66**, (1), pp. 5–18
[16] Weickert J.: 'Anisotropic diffusion in image processing' (University of Copenhagen Denmark Press, 1998)
[17] Yahya A.A., Tan J., Hu M.: 'A blending method based on partial differential equations for image denoising', *Multimedia Tools Appl.*, 2014, **73**, (3), pp. 1843–1862
[18] Tikhonov A.N., Arsenin V.Y.: 'Solutions of ill-posed problem' (Winston and Sons, Washington, DC, 1977)
[19] Andreu F., Mazón J.M., Moll J.S.: 'The total variation flow with non-linear boundary conditions', *Asymptotic Anal.*, 2005, **43**, (1-2), pp. 9–46
[20] Chono K., Senda Y.: 'Enhanced reconstruction of AVC/H.264 intra video based on motion compensated temporal filtering and total-variation regularization'. Proc. of IEEE Picture Coding Symp., 2009, pp. 1–4
[21] Liu J., Gao F., Li Z.: 'A model of image denoising based on partial differential equations'. Proc. of IEEE Int. Conf. on Multimedia Technology (ICMT), 2011, pp. 1892–1896
[22] Yahya A.A., Tan J., LI L., *ET AL.*: 'A hybrid method of image denoising based on the isotropic diffusion and total variation models', *J. Comput. Inf. Syst.*, 2015, **11**, (3), pp. 1149–1161